Received: 12 December 2019 | Revised: 5 February 2020 | Accepted: 6 February 2020

DOI: 10.1002/pol.20190274

ORIGINAL ARTICLE

JOURNAL OF POLYMER SCIENCE WILEY

Quantitative nanoscale measurements of the thermomechanical properties of poly-ether-ether-ketone (PEEK)

Wen Qian[1] | **Wenlong Li**[1] | **Charles Nguyen**[1] | **Tyler J. Johnson**[2] | **Joseph A. Turner**[1]

[1]Department of Mechanical & Materials Engineering, University of Nebraska-Lincoln, Lincoln, Nebraska

[2]Department of Chemical & Biomolecular Engineering, University of Nebraska-Lincoln, Lincoln, Nebraska

Correspondence
Wen Qian and Joseph A. Turner, Department of Mechanical & Materials Engineering, University of Nebraska-Lincoln, Lincoln, NE 68588.
Email: wqian2@unl.edu (W. Q.) and jaturner@unl.edu (J. A. T.)

Funding information
Nebraska Research Initiative

Abstract

Understanding the internal structure and organization of semicrystalline polymers, especially at the nanoscale, has many challenges for researchers to date. In this article, we demonstrate a quantitative method for investigating the local viscoelastic properties (i.e., storage and loss moduli, as well as loss tangent) of semicrystalline polyether-ether ketone (PEEK) through the combination of contact resonance atomic force microscopy (CR-AFM) and in situ local heating with a thermal probe. Furthermore, the local viscoelastic properties of the crystalline and amorphous phases were decoupled by performing thermal CR-AFM array mapping near the glass transition temperature of PEEK (T_g, 143 °C). A distinct bimodal distribution of tip-sample interaction was observed for PEEK near its T_g, providing a means to estimate the T_g and the degree of crystallinity of PEEK.

KEYWORDS

atomic force microscope, contact resonance, local probe heating, localized mechanical property, PEEK

1 | INTRODUCTION

Macroscale mechanical and thermal properties of polymers have been heavily investigated in the past. Current challenges in the understanding of polymer behavior at the nanoscale has piqued great interest from researchers, but many questions remain due to the inherent difficulty of investigating polymers at this length scale. Furthermore, semicrystalline polymers at the nanoscale exhibit localized distributions of amorphous and crystalline phases, complicating the characterization of their nanoscale thermomechanical properties. Poly-ether-ether-ketone (PEEK) is a semicrystalline thermoplastic with a glass transition temperature (T_g) of 143 °C, rivaling most other polymers in terms of its high strength-to-weight ratio and excellent biocompatibility.[1,2] During the past few decades, the thermomechanical properties of PEEK have been studied using various approaches including mechanical testing,[3,4] thermal analysis,[5,6] differential scanning calorimetry (DSC),[7,8] X-ray diffraction (XRD),[9,10] instrumented indentation,[11,12], and modeling.[13,14] Although these characterization methods were used to study the mechanical properties and internal structure of PEEK on the macroscale, the dynamic mechanical properties at the nanoscale as a function of temperature, as well as the intrinsic localized distribution of amorphous and crystalline structures, have not been investigated yet.

Atomic force microscopy (AFM) is a characterization technique that is well-known for its nanoscale spatial resolution with tip radius as low as several nanometers. Contact resonance atomic force

microscopy (CR-AFM) is a dynamic, in-contact adaptation of AFM that exploits the mechanical vibration response of an AFM cantilever to probe mechanical properties by sensing the resonance frequency of the AFM cantilever which is oscillating on the test sample. The resulting measurement comprises the vibrational response of the cantilever-sample interaction. A constitutive linear viscoelastic model (Voigt model) is employed to quantify the tip-sample interaction. As a result, CR-AFM can be used to quantify the local viscoelastic properties of materials at the nanoscale.[15–19] A unique adaptation of the CR-AFM method, which utilizes a U-shaped thermal cantilever instead of a conventional, single-beam rectangular cantilever, has been investigated by our group in the past.[20,21] The shape of the cantilever allows it to be actuated using the Lorentz force, allowing for cleaner signals in both vertical and lateral motion. This configuration of the cantilever also boasts the ability to pass a current through the U-shaped portion (the legs) which causes local heating. This probe, the Thermalever™, permits investigation of the localized mechanical properties and phase transition as a function of temperature.[22–24] Because the sample is locally heated, the material response is confined only to the contact region between the heated probe tip and the substrate, allowing for the specific nanoscale interphase regions and phase transition to be examined while leaving the remainder of the bulk unperturbed.

Current methods of determining the T_g of polymers (especially semicrystalline polymers) lack the ability to quantify it at the nanoscale. Several articles report T_g detection through nanoscale thermal analysis,[23,25–29] including monitoring the probe displacement, monitoring the changes of thermal impedance, or comparing the phase image contrast.

When a semicrystalline material is heated up to or above its T_g, the viscosity of the amorphous portion normally decreases while the mechanical behavior of the crystalline portion remains relatively constant. Therefore, the mechanical response of two phases can be decoupled and can be detected by using the localized thermal CR-AFM technique. In this manuscript, we demonstrate the effectiveness of thermal CR-AFM for quantifying the dynamic mechanical properties of semicrystalline PEEK at the nanoscale for various temperatures. In addition, the localized thermal dependence of the storage modulus (E') and loss modulus (E'') are quantified. Thermal CR-AFM can be used to determine the T_g by detecting the change in viscosity as a function of temperature, and can also be used to differentiate the crystalline phase from the amorphous phase for PEEK through array mapping. [15]

2 | EXPERIMENTAL

2.1 | PEEK sample treatment

A 12.7 mm VICTREX PEEK 450G plate was purchased from the Victrex Company. A small strip of $10 \times 10 \times 5$ mm^3 was cut from the plate and annealed in a vacuum oven at 280 °C for 12 hr and then subsequent cooling to reorganize the chains of the crystalline phase, thereby to increase the crystallinity degree. After annealing, the outer sample surface was removed using a diamond saw. The sample was then polished using a 1,000 grit (~18 μm) sand paper, followed by a medium polishing using 1 μm liquid emulsion polishing compound (Al_2O_3) and a fine polishing using 0.05 μm liquid emulsion polishing compound (Buehler, Al_2O_3).

2.2 | Thermal CR-AFM measurement

All CR-AFM spectra and array mapping were collected on the Anasys afm + (Anasys Instruments, Santa Barbara, CA) with a Thermalever™ probe model AN2-300. This probe can achieve maximum temperatures of up to 400 °C, with a first free vibrational resonance frequency range of 20–35 kHz and spring constant $k_c \sim 0.35$ N m^{-1}. Nominal geometrical data for the cantilever used were ~ $300 \times 50 \times 2$ μm^3 (length × width × thickness) with a tip height ~ 5 μm. A 10×10 measurement array within an area of 5×5 μm^2 was used. Frequency sweeps (100–180 kHz) were performed on the sample at temperatures of 30, 80, 100, 120, 140, 150, 160, 170, and 180 °C.

2.3 | Structural and property measurements

Fourier transform infrared (FT-IR) absorption spectra were obtained in the wavenumber range from 400–4,000 cm^{-1} with 2 cm^{-1} resolution using a Nicolet™ iS50 FTIR Spectrometer in ATR mode. X-Ray diffraction (XRD) pattern measurements of the sample were performed in the 2θ range of 15–50° using a Rigaku Ultima IV XRD system with graphite monochromatized Cu Kα radiation ($\lambda = 1.54187$ Å). Crystallinity degree was calculated by dividing the total area of crystalline peaks by the total area under the diffraction curve. Particle sizes were estimated using the full-width at half-maximum (FWHM) of XRD peaks according to the Scherrer law. The morphology and crystal shape of PEEK were observed by field-emission scanning electron microscope (FESEM, FEI Helios Nanolab 660). The glass transition

temperature of the bulk PEEK annealed sample was measured using a Netzsch DSC Phoenix 204 F1. A nitrogen flow rate of 50 mL/min was used. The 13.72 mg sample was placed in an aluminum pan, and purged with nitrogen gas with a flow rate of 50 mL/min. The sample was first heated from 30 to 450 °C at a heating rate of 5 K/min, and then was kept at 375 °C for 1 min to allow complete melting. Finally, it was cooled to 30 °C at a cooling rate of 5 K/min. Nano-dynamic mechanical analysis (nano-DMA) testing was performed at room temperature with frequency sweeps from 100 to 0.1 Hz with 12 steps on logarithmic scale using a Hysitron TI 950 Triboindenter. The mass density of the sample at room temperature was evaluated by measuring the sample weight in distilled water and in air using a balance (Mettler Toledo AT201).

3 | RESULTS AND DISCUSSION

3.1 | Thermal CR-AFM measurements

CR-AFM measurements were made using the Anasys afm+. A U-shaped Thermalever™ probe was used for these measurements (Figure 1a). These probes incorporate a doped silicon resistive heater at the end of the probe (far away from the tip) which allows for reliable heating to temperatures up to 400 °C. The U-shaped cantilever is actuated by passing a sinusoidal current through it in the presence of a magnetic field, resulting in a perpendicular motion of the cantilever via the Lorentz force. First, the AFM cantilever is oscillated freely, above the test sample, and a measurement is collected (Figure 1b). Next, the cantilever is brought into contact with the test sample, and a measurement of the cantilever-sample coupled response is collected (Figure 1c). When the AFM tip is in contact with sample surface, the resonances shift to higher frequencies (Figure 1d). The relative frequency shift of each resonance is used to determine an equivalent contact stiffness and damping between the AFM tip and the sample. The dispersive, nonlinear equations governing the resonant frequencies and tip-sample interaction, along with the equations used to quantify viscoelastic properties, are discussed in Data S1.

To confirm that no contaminants were created from the sample polishing process, we performed FT-IR analysis as shown in (Figure S1). We also performed X-ray diffraction (XRD) analysis and used the Scherrer equation to calculate the average size of the crystallites, which is around 14 nm (Figure S2a). The SEM image (Figure S2b) of the sample shows the crystal size is within the range of 10–20 nm, consistent with XRD results. A 10 × 10 array of positions covering a scan area of 5 × 5 μm^2, measured

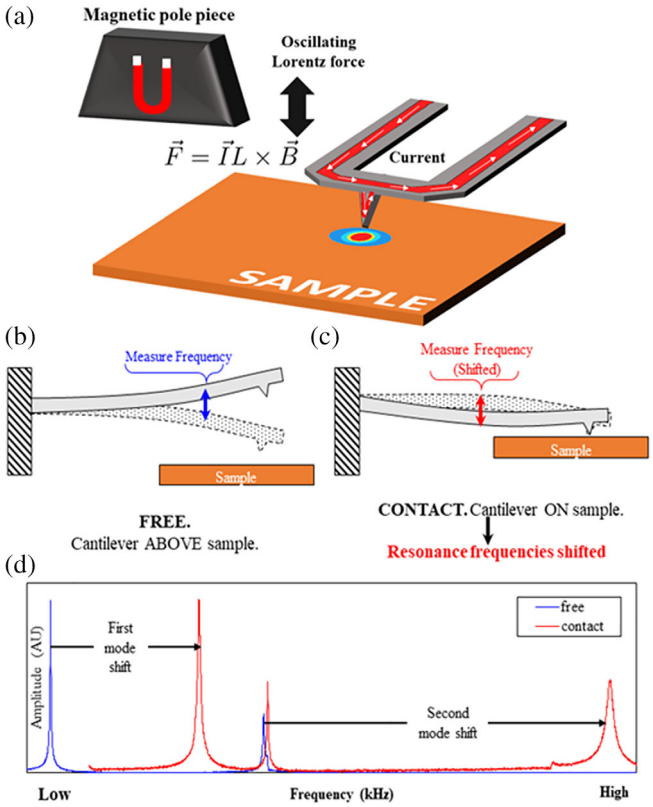

FIGURE 1 (a) Diagram showing the key features of Lorentz contact-resonance AFM and thermal AFM through local heating, (b) AFM cantilever vibration at free mode, (c) AFM cantilever vibration at contact mode, and (d) contact resonance spectrum shifts from free mode to contact mode [Color figure can be viewed at wileyonlinelibrary.com]

for several temperatures, was performed on PEEK using thermal CR-AFM. Each spot size is approximately 50 nm in diameter due to the tip radius of the probe. For each temperature, the 100 total measurements were plotted as histograms to illustrate the distribution of the measured contact resonance frequencies.[15] Figure 2a,b shows the CR-AFM spectra measured at 30 and 140 °C, respectively. At 30 °C, a narrow distribution of the peak positions was observed (Figure 2a). The most prominent resonance frequency is located slightly above 134 kHz, as shown in the histogram (Figure 2c). However, at 140 °C, a distinctly bimodal distribution of the resonance frequencies was observed (Figure 2b). The histogram (Figure 2d) shows 40 spectra that have a resonance frequency distribution slightly above 134 kHz, while the remaining 60 resonances were distributed slightly above 131 kHz. We assume that the change of stiffness of the cantilever due to the increase in temperature is negligible in comparison to PEEK near its T_g. Therefore, because a decrease in the resonance frequency indicates a decrease in the tip-sample stiffness interaction, the observed decrease in

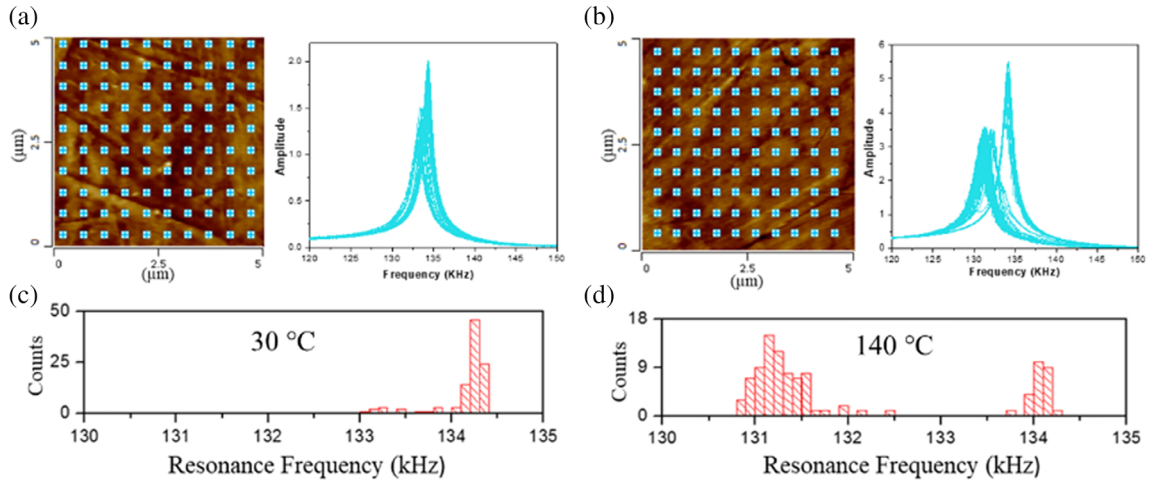

FIGURE 2 (a and b) CR-AFM spectrum of PEEK at 30 and 140 °C, respectively, with 10 by 10 array in the scan area of 5 × 5 μm^2; (c and d) the statistical histogram plots of peak frequency at 30 and 140 °C, respectively [Color figure can be viewed at wileyonlinelibrary.com]

resonance frequency is attributed to the "softening" of PEEK. It is well-known that when the temperature of a semicrystalline polymer is close to its T_g, the viscosity of the amorphous component is significantly reduced, but the crystalline component changes very little.[11] Thus, the appearance of the lower resonance frequency distribution near 131 kHz at 140 °C is attributed to the decay of "labile oxygen related functionalities" onset of T_g, causing the molecules movement having enough energy to overcome the resonance-stabilization from the ether linkages.[30] The distribution near 134 kHz at 140 °C is attributed to the crystalline regions because these are not significantly affected by the increase in temperature. By counting the number of measurements associated with each distribution, the results indicate that the crystallinity degree of the sample surface is around 40%, just slightly greater than the bulk crystallinity degree estimated by XRD (36.42%, Data S1).

It is worth noting that the bimodal resonance frequency response of the PEEK at 140 °C shows not only the presence of two distinct phases, but also the variation of the tip-sample interaction stiffness of these two phases. Because the crystalline size is less than 20 nm while the CR-AFM spot size is 50 nm, it is possible that each individual measurement in the array includes both crystalline and amorphous contributions to the tip-sample interaction. We assume that the observed mechanical response represents the dominant phase in the tested location. As the temperature approaches T_g, the detected resonant frequency would remain constant if the crystalline component is dominant. On the contrary, if the amorphous component is dominant and the temperature is near T_g, the measurement will show a more compliant mechanical response, causing the resonance frequency to shift lower. To the best of our knowledge, localized variations of T_g cannot be detected by other global, or macroscale measurement techniques. The 10 × 10 array map provides an effective quantitative method to distinguish the amorphous and crystalline domains with nanoscale spatial resolution.

3.2 | Frequency and FWHM histogram of array mapping measurement

To investigate the phase distribution of PEEK and the nature of the tip-sample interaction in more detail, CR-AFM was performed at several temperatures between 30 and 180 °C. Figure 3a shows the frequency histogram obtained from the CR-AFM spectra (Figures S3-S7) at 30°C and elevated temperatures from 80 to 140 °C in steps of 20 °C. Figure 3b shows the frequency histogram obtained from the CR-AFM spectra (Figures S7-S11) at elevated temperatures from 140 to 180 °C in steps of 10 °C. As the temperature increased from 30 to 140 °C, the distribution near 134 kHz (Indicating the "crystalline-like" regions) remains present while the distribution near 131 kHz (indicating the "amorphous-like" regions) gradually appears due to the PEEK transitioning to a more rubbery-like state. When the temperature increases above 140 °C, up to 180 °C, the "crystalline-like" distribution remains, but the "amorphous-like" distribution gradually disappears. A similar histogram which shows the full width at half maximum (FWHM) of the frequency response spectra is shown in Figure 4a-b. Briefly, the FWHM is a value that is related to the tip-sample damping interaction and is indicative of viscous contributions to the mechanical response (see Data S1). As the

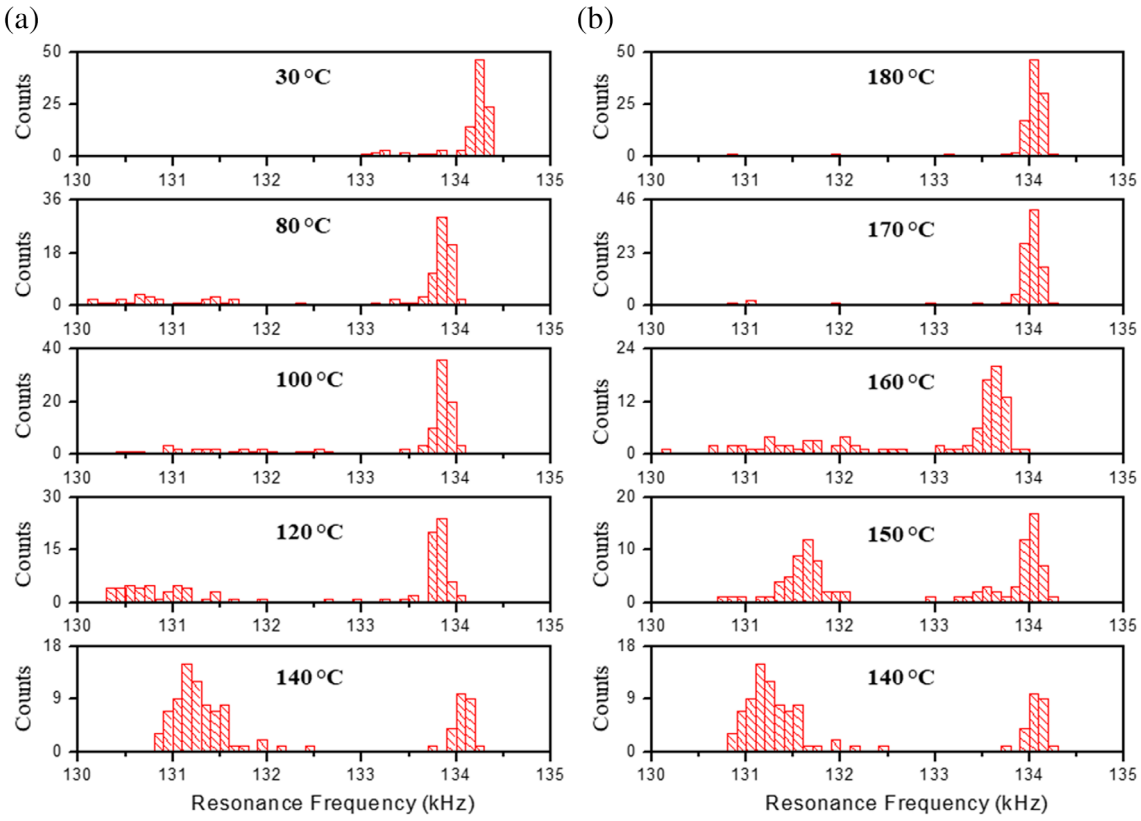

FIGURE 3 Frequency histograms of 10 by 10 array peak frequency of CR-AFM spectrum at elevated temperatures, (a) from 30 to 140 °C and (b) from 140 to 180 °C [Color figure can be viewed at wileyonlinelibrary.com]

temperature increased from 30 to 140 °C, the distribution of FWHM values broadens, indicating the increasing observation of more "amorphous-like" tip-sample interaction. Notably, when the temperature increases from 140 to 180 °C, the distribution of FWHM values gradually narrows, indicating the increasing observation of more "crystalline-like" tip-sample interaction.

The ostensible "disappearance" of the amorphous regions in the observed measurements of PEEK above its T_g can be reasonably explained. While below T_g, the amorphous regions of the semicrystalline polymer are entangled. This entanglement prevents significant chain motion in the amorphous regions, making it difficult to decouple the mechanical behaviors of two phases. As a result, the tip-sample interaction is dominated by the "crystalline-like" response. As the temperature nears T_g, the amorphous regions begin to untangle, chain motion increases, and the local stiffness decreases. The onset of this phenomena is detectable by CR-AFM as the appearance of a resonance frequency distribution that is attributed to the "amorphous-like" regions. Finally, when the temperature increases beyond T_g, the amorphous regions of the polymer become rubbery, resulting in a negligible contribution to the dominant mechanical response of the tip-sample interaction. As a result, only the "crystalline-like" response is observed. Additionally, while under T_g, there is little or no penetration of the tip into the sample. However, above T_g, the heated AFM tip creates plastic deformations in the surface. We observed that tip penetration depth increased from ~15 nm to ~30 nm when the temperature increased from 160 to 180 °C (Figures S12–14), which is due to both the softening of the surface and adhesion effects. [31,32] In order to examine the consistency of these results, we have repeated the CR-AFM measurements in different areas at the same temperatures of 140, 150, and 160 °C, as shown in Figure S15. The repeated measurements on different areas are similar and consistent.

3.3 | Mechanical model for contact resonance spectrum

An AFM cantilever beam (with cross-sectional area A, Young's modulus E, bending moment of inertia I, damping of the beam χ, density of the beam ρ) in contact with a viscoelastic surface is modeled as shown in Figure 5a-b where $q(x,t)$ is the displacement along the cantilever at time t. In most cases, the AFM cantilever is installed with a small angle ($\theta_0 \sim 15°$).[33] For simplicity, the AFM cantilever is

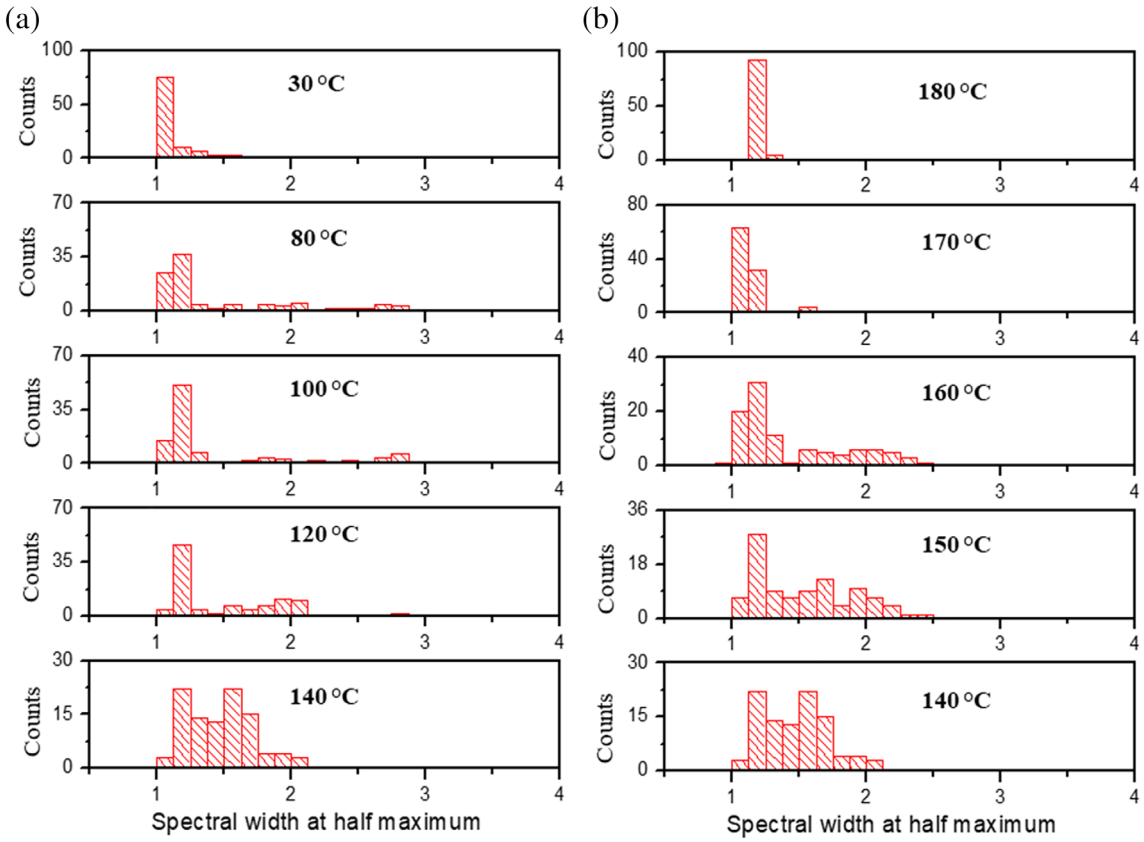

FIGURE 4 Statistical histogram plots of 10 by 10 array FWHM of CR-AFM spectrum at elevated temperatures, (a) from 30 to 140 °C and (b) from 140 to 180 °C [Color figure can be viewed at wileyonlinelibrary.com]

assumed here to be parallel to the sample surface when engaged ($\theta_0 \sim 0°$). The cantilever beam is also considered to be of rectangular shape with width w, thickness b, and total length L_T.[34,35] The AFM cantilever tip-sample interaction is modeled as a spring with stiffness k and a dashpot with damping coefficient, c in a parallel configuration. In CR-AFM, spectra are obtained from a non-contact case (also known as the free case) and a contact case to obtain frequency spectra f_n^0 and f_n^C, respectively. The spectra from the free case and the contact case also contain the free and contact resonance quality factors Q_n^0 and Q_n^C, for the nth flexural eigenmode, which are then used to determine viscoelastic properties of storage modulus E' and loss modulus E''. Additional discussion of the mechanical model is presented in Data S1.

3.4 | Local storage and loss modulus analysis of crystalline and amorphous phases

Using the mechanical model, an in-house program to analyze the frequency response of CR-AFM data, intelligent contact resonance AFM for viscoelasticity (iCRAVE), was developed to evaluate the frequency response of the probe and PEEK. iCRAVE was used to determine local storage modulus of the two distinct phases at different temperatures from 80 to 160 °C, as shown in Figure 6a. At 80 °C, average $E'_{\text{“amorphous-like”}} = 1.399 \pm 0.123$ GPa, average $E'_{\text{“crystalline-like”}} = 2.494 \pm 0.075$ GPa; at 140 °C, average $E'_{\text{“amorphous-like”}} = 1.335 \pm 0.089$ GPa, average $E'_{\text{“crystalline-like”}} = 2.442 \pm 0.116$ GPa. These results show that the average value of local storage modulus for “crystalline-like” (2.4–2.5 GPa) and “amorphous-like” (1.3–1.4 GPa) phase are stable and have little variation at different temperatures. Furthermore, we acquired local loss modulus of the two distinctive phases at different temperatures from 80 to 160 °C, as shown in Figure 6b. At 80 °C, average $E''_{\text{“amorphous-like”}} = 0.058 \pm 0.017$ GPa, average $E''_{\text{“crystalline-like”}} = 0.037 \pm 0.003$ GPa; at 100 °C, average $E''_{\text{“amorphous-like”}} = 0.078 \pm 0.012$ GPa, average $E''_{\text{“crystalline-like”}} = 0.041 \pm 0.005$ GPa. These results show that the average values of local loss modulus for “crystalline-like" phase are still very stable within the narrow range of 0.035–0.041 GPa at different temperatures, but the local loss modulus of “amorphous-like" phase has a variation from 0.045 to 0.078 GPa. In addition, we also acquired the average storage modulus values with uncertainty (Figure 6c) for the 10 × 10 arrays

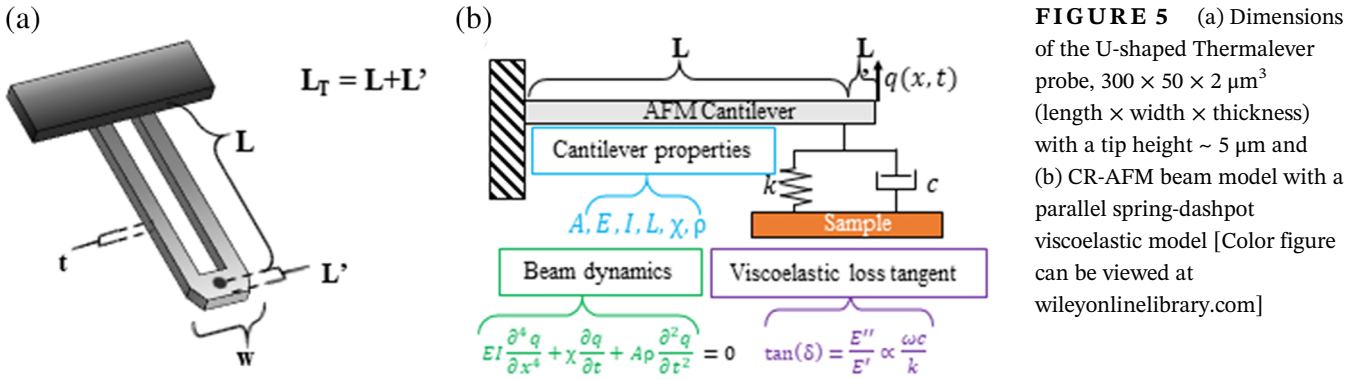

FIGURE 5 (a) Dimensions of the U-shaped Thermalever probe, 300 × 50 × 2 μm^3 (length × width × thickness) with a tip height ~ 5 μm and (b) CR-AFM beam model with a parallel spring-dashpot viscoelastic model [Color figure can be viewed at wileyonlinelibrary.com]

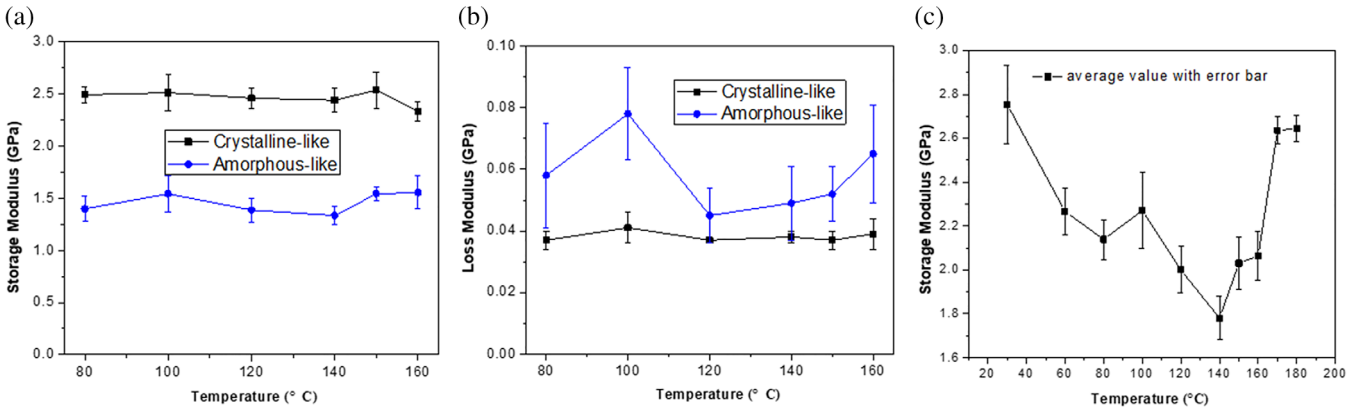

FIGURE 6 (a) The average values of local storage modulus of the "crystalline-like" and "amorphous-like" phases at different temperatures, respectively, (b) the average values of local loss modulus of the "crystalline-like" and "amorphous-like" phases at different temperatures, respectively, and (c) the average storage modulus values of a total 100 spots at different temperatures [Color figure can be viewed at wileyonlinelibrary.com]

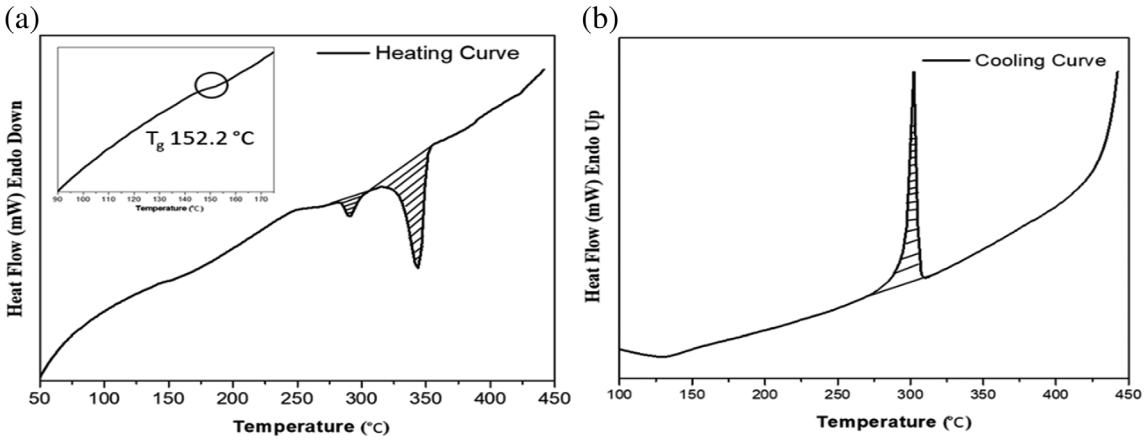

FIGURE 7 (a and b) DSC heating curve and cooling curves of sample, respectively

at different temperatures. For the results at each temperature, a weighted average was calculated based on the percentage of positions that exhibit the two types of behavior. For example, if a 10 × 10 array included 73 "amorphous-like" spectra and 27 "crystalline-like" spectra, the weighted average storage modulus is given by $E'_{\text{Ave}} = 0.73E'_{\text{"amorphous-like"}} + 0.27E'_{\text{"crystalline-like"}}$. The minimum value of the weighted-average storage modulus was observed for a temperature of 140 °C, indicating the presence of a glass transition of PEEK.

To determine the accuracy of the T_g information obtained by thermal CR-AFM, we also performed differential scanning calorimeter (DSC) measurements to investigate the glass transition temperature of PEEK. The DSC heating and cooling curves are shown in Figure 7a,b. The melting temperature T_m for the sample is around 350 °C. The T_g for the bulk sample is around 152.2 °C, as highlighted with a circle in Figure 7a (inset), a value that is 8.57% higher than T_g (140 °C) measured at the nanoscale by thermal CR-AFM. We also performed dynamic mechanical analysis (DMA) on PEEK at the frequency of 1 Hz for time–temperature superposition (TTS) analysis. As shown in Figure S16, the peak value of T_g is around 160 °C from these measurements. Differences of T_g between bulk and local scales has already been confirmed by refined modeling.[36] In addition, the degree of crystallinity can also be obtained by integrating the area under the melting peak (37.10 J/g) and crystallization peak (37.94 J/g) during the heating and cooling cycles, respectively. The integration is normalized to the actual weight fraction of PEEK sample and then divided the area by the heat of fusion of 100% crystalline PEEK (130 J/g).[37] The crystallinity degree was calculated to be 32.56%, which is similar with our density measurement results (33.65%), as shown in Table S1.

4 | CONCLUSIONS

In summary, we employed a unique and effective technique by using CR-AFM and local heating to quantify the localized viscoelastic properties of PEEK. We demonstrated that CR-AFM has the capability to differentiate the crystalline and amorphous phases, to estimate T_g and to investigate the crystallinity degree at nanoscale. This approach also quantified the localized storage and loss moduli, at elevated temperatures via the iCRAVE analysis code. In ongoing work, iCRAVE will be further developed and optimized to support the modeling of a U-shaped probe, which is capable of shear modulus measurement at the nanoscale, and the local thermal CR-AFM technique will be optimized for other semicrystalline polymers.

ACKNOWLEDGMENTS

Manufacturing and characterization analysis were performed at the NanoEngineering Research Core Facility (NERCF), which is partially funded by the Nebraska Research Initiative. Modeling work is supported by Nebraska Center for Energy Sciences Research (NCESR).

ORCID

Wen Qian https://orcid.org/0000-0001-5813-7817

REFERENCES

[1] D. P. Jones, D. C. Leach, D. R. Moore, *Polymer* **1985**, *26*, 1385.
[2] S. Hamdan, G. M. Swallowe, *J. Mater. Sci.* **1996**, *31*, 1415.
[3] P. J. Rae, E. N. Brown, E. B. Orler, *Polymer* **2007**, *48*, 598.
[4] Z. Zhang, C. Breidt, L. Chang, K. Friedrich, *Tribol. Int.* **2004**, *37*, 271.
[5] A. G. Al Lafi, J. N. Hay, D. J. Parker, *J. Polym. Sci. Part B-Polym. Phys.* **2008**, *46*, 2212.
[6] W. Li, G. Gazonas, E. N. Brown, P. J. Rae, M. Negahban, *Mechanics of Materials* **2019**, *129*, 113.
[7] Y. Kong, J. N. Hay, *Polymer* **2002**, *43*, 3873.
[8] T. X. Liu, Z. S. Mo, S. G. Wang, H. F. Zhang, *Polym. Eng. Sci.* **1997**, *37*, 568.
[9] R. Verma, H. Marand, B. Hsiao, *Macromolecules* **1996**, *29*, 7767.
[10] S. S. Tan, A. H. Su, J. Luo, E. L. Zhou, *Polymer* **1999**, *40*, 1223.
[11] G. Z. Voyiadjis, A. Samadi-Dooki, L. Malekmotiei, *Polym. Test* **2017**, *61*, 57.
[12] A. Molazemhosseini, H. Tourani, M. R. Naimi-Jamal, A. Khavandi, *Polym. Test* **2013**, *32*, 525.
[13] Y. Y. Li, V. Agrawal, J. Oswald, *J. Polym. Sci. Part B-Polym. Phys.* **2019**, *57*, 331.
[14] B. N. Chang, X. Y. Wang, Z. Q. Long, Z. Li, J. F. Gu, S. L. Ruan, C. Y. Shen, *Polym. Test* **2018**, *69*, 514.
[15] H. Wagner, D. Bedorf, S. Küchemann, M. Schwabe, B. Zhang, W. Arnold, K. Samwer, *Nat. Mater.* **2011**, *10*, 439.
[16] K. Yamanaka, S. Nakano, *Jpn. J. Appl. Phys. Part 1 – Regul. Pap. Short Notes Rev. Pap.* **1996**, *35*, 3787.
[17] U. Rabe, K. Janser, W. Arnold, *Rev. Sci. Instrum.* **1996**, *67*, 3281.
[18] U. Rabe, S. Amelio, E. Kester, V. Scherer, S. Hirsekorn, W. Arnold, *Ultrasonics* **2000**, *38*, 430.
[19] U. Rabe, S. Amelio, M. Kopycinska, S. Hirsekorn, M. Kempf, M. Göken, W. Arnold, *Surf. Interface Anal.* **2002**, *33*, 65.
[20] E. Rezaei, J. A. Turner, *J. Appl. Phys.* **2014**, *115*, 174302.
[21] E. Rezaei, J. A. Turner, *J. Appl. Phys.* **2016**, *119*, 034303.
[22] B. Lee, C. B. Prater, A. P. King, *Nanotechnology* **2012**, *23*, 055709.
[23] B. A. Nelson, W. P. King, *Rev. Sci. Instrum.* **2007**, *78*, 023702.
[24] S. Jesse, M. P. Nikiforov, L. T. Germinario, S. V. Kalinin, *Appl. Phys. Lett.* **2008**, *93*, 073104.
[25] J. Chen, D. C. Yang, *Macromolecules* **2005**, *38*, 3371.
[26] V. V. Tsukruk, V. V. Gorbunov, N. Fuchigami, *Thermochim. Acta* **2002**, *395*, 151.
[27] D. S. Fryer, P. F. Nealey, J. J. de Pablo, *Macromolecules* **2000**, *33*, 6439.
[28] C.-C. Lin, K.-H. Chang, K.-C. Lin, W.-F. Su, *Compos. Sci. Technol.* **2009**, *69*, 1180.
[29] M. J. Fasolka, A. M. Mayes, S. N. Magonov, *Ultramicroscopy* **2001**, *90*, 21.
[30] M. Vinothkannan, A. R. Kim, K. S. Nahm, D. J. Yoo, *RSC Adv.* **2016**, *6*, 108851.
[31] T.-H. Fang, C.-D. Wu, S.-H. Kang, *Micron* **2011**, *42*, 492.
[32] B. Cappella, W. Stark, *J. Colloid Interface Sci.* **2006**, *296*, 507.
[33] U. Rabe, J. Turner, W. Arnold, *Appl. Phys. A* **1998**, *66*, S277.
[34] P. A. Yuya, D. C. Hurley, J. A. Turner, *J. Appl. Phys.* **2008**, *104*, 074916.
[35] P. A. Yuya, D. C. Hurley, J. A. Turner, *J. Appl. Phys.* **2011**, *109*, 113528.

[36] L. Jin, J. Ball, T. Bremner, H. J. Sue, *Polymer* **2014**, *55*, 5255.
[37] X. Tardif, B. Pignon, N. Boyard, J. W. P. Schmelzer, V. Sobotka, D. Delaunay, C. Schick, *Polym. Test* **2014**, *36*, 10.

SUPPORTING INFORMATION

Additional supporting information may be found online in the Supporting Information section at the end of this article.

How to cite this article: Qian W, Li W, Nguyen C, Johnson TJ, Turner JA. Quantitative nanoscale measurements of the thermomechanical properties of poly-ether-ether-ketone (PEEK). *J Polym Sci*. 2020;58:1544–1552. https://doi.org/10.1002/pol.20190274